The Influence of Molecular Weight on the Surface Properties of Polyelectrolyte Multilayers

Major Qualifying Project completed in partial fulfillment of the Bachelors of Science Degree in Chemical Engineering at Worcester Polytechnic Institute, Worcester, MA

Submitted by: Elizabeth Towle

Professor Amy Peterson, Faculty Advisor

Abstract

Polyelectrolyte multilayers (PEMs), thin polymer films assembled from polyelectrolytes, are most commonly used as a coating to modify the surface properties of a bulk material, making the optimization of surface properties critical. In this study, the influence of polyelectrolyte molecular weight was examined, as well as the assembly pattern that each molecular weight produces. PEMs were created with poly(acrylic acid) (PAA) and poly-l-lysine (PLL) at low, medium, and high molecular weight to determine the effects of molecular weight on the surface properties of PEMs, specifically surface free energy (SFE) and roughness. Molecular weight has a significant impact on the assembly pattern and therefore the surface properties. Low MW PAA and PLL were found to form less massive PEMs composed primarily of PLL, while high MW PEMs had high mass and more PAA than PLL. Medium MW PEMs had the most linear assembly pattern and were the most balanced between polyelectrolytes. Medium MW PEMs were the smoothest, and had the lowest SFE, while low MW PEMs were the roughest and had the highest SFE. However, high MW PEMs were also quite rough while having a low SFE similar to that of the medium MW PEMs. While further research will be needed to understand how prevalent this specific pattern is with other polyelectrolyte combinations, these results demonstrate the tunability of surface properties including SFE and roughness with molecular weight.

Table of Contents

Table of Figures

Table of Tables

1. Introduction

The assembly of polyelectrolytes into thin polymer films referred to as polyelectrolyte multilayers (PEMs) has become an important topic of study since its introduction 25 years ago.[1] PEMs can be designed to have a wide variety of properties by adjusting various assembly parameters.[2] Due to their versatility, PEMs can be designed for a myriad of applications, including biosensors,[3] encapsulation,[4] and drug delivery.[5] PEMs are most commonly used as a coating to modify the surface properties of a bulk material, making the optimization of surface properties critical.[6] This research endeavor explored the influence of polyelectrolyte molecular weight on surface properties including roughness and surface free energy (SFE) to allow for greater prediction and control of PEM surface properties.

In this study, the influence of polyelectrolyte molecular weight was examined, as well as the assembly pattern that each molecular weight produces.[2,7] PEMs were created with poly(acrylic acid) (PAA) and poly-l-lysine (PLL) at three MWs to form low, medium, and high MW PEMs. The first aim of this research endeavor was to assess the assembly pattern produced by each set of molecular weights to ascertain a model of each PEM. The assembly of these PEMs was characterized using spectroscopic ellipsometry to evaluate thickness and quartz crystal microbalance with dissipation monitoring to determine mass accumulation as well as stiffness. Additionally, thickness and mass were used to determine a relative density of each PEM. The next aim was to use these multilayers to assess the effects of molecular weight on the surface properties of PEMs. Therefore, SFE and roughness were measured with goniometry and atomic force microscopy, respectively.

Each molecular weight produced a different assembly pattern, including different total mass and ratio of polyelectrolytes, which affected the properties of each PEM. The PEMs with the lowest MW polyelectrolytes (low MW PEMs) were the least massive and exhibited stripping by PAA. The PEMs formed by the highest MW polyelectrolytes (high MW PEMs) were the most massive and showed some stripping in the final bilayer by PLL. This stripping was the culmination of a pattern in high MW PEMs where the mass of PAA added each layer rose while additions by PLL declined. PEMs composed of medium MW polyelectrolytes (medium MW PEMs) were more consistent in their assembly, exhibiting a relatively linear growth pattern and a consistent ratio of polyelectrolytes.

Medium MW PEMs were found to be the smoothest, which may be attributable to this consistent assembly pattern. All PEMs increased in roughness as more layers were added, though not in a linear manner. Low MW PEMs were found to be the roughest. The total SFE of the low MW PEMs was found to be the highest, primarily attributable to a high basic component. Overall, medium MW PEMs had the lowest SFE, but were closely followed by the high MW PEMs.

These results suggest that, for PAA-PLL PEMs, there may be an ideal mid-range MW that will form the most consistent PEMs, allowing for smooth, low energy surfaces. Rougher surfaces with a high surface energy, especially in the basic component, can be created by using lower MW polyelectrolytes. High MW polyelectrolytes can be used to form rough low energy surfaces.

Additional research will be needed to determine if other polyelectrolyte combinations exhibit the same trend. Further research could also identify the specific range which produced these smooth low energy PEMs for PAA/PLL, as well as other polyelectrolytes.

2. Background

2.1 Polyelectrolyte Multilayers

PEMs are a form of polymer film that can be created from alternating layers of polyanions and polycations built up layer by layer. This assembly process allows for the creation of films between several angstrom and micrometers thick, with experimental control of the structure and properties possible for each layer.[6] PEMs have been investigated for their usefulness in a wide variety of applications including biosensors,[3] encapsulation,[4] and drug delivery.[5] To optimize PEMs for these various applications, it is imperative to understand their assembly and how the process can be modified to manipulate the eventual properties of the films.

In 1992, the method of creating PEMs was detailed by Decher et al. as a process of dipping a positively charged planar surface in an aqueous solution of anionic polyelectrolytes, followed by alternating immersions in polycation and polyanion solutions with water rinses between.[1] This is referred to as layer-by-layer (LbL) assembly, and allows for careful control of the thickness of the multilayer film. It has since been demonstrated that irregular surfaces can also be coated, including spheres and capsules.[8,9] The formation of PEMs was initially believed to driven by electrostatic interactions,[6] as the charge often inverts as each layer is added. However, PEMs can be formed without this alternating pattern in the sign of the surface potential.[10] von Klitzing et al. proposed an increase in entropy due to the release of counterions as an alternative driving force, which has been subsequently confirmed by others.[2]

PEMs are useful in various thin film applications due to several important properties. Their shape is not limited in any way, as formation by dip coating allows them to conform to the shape of the surface provided. Further, the LbL nature of this assembly allows for manipulation of individual layers.[2] The properties of each layer can be adjusted or functional layers of nanoobjects can be incorporated, including molecular aggregates, clusters or colloids.[6] Additionally, the thickness of a PEM can be designed with angstrom precision.[2] This versatility makes PEMs useful for a wide variety of applications. Most PEMs are designed for biomedical purposes, as many of the polyelectrolytes studied are biocompatible in various conditions and can be coated onto less compatible structures. These applications include biosensors,[3] encapsulation,[4] and drug delivery.[5] PEM coatings can also be used to adjust hydrophilicity,

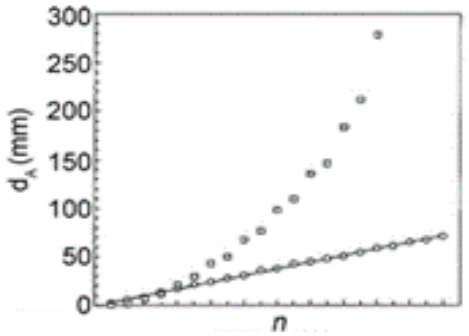

Figure 1: Exponential and linear growth modes in low and high molecular weight PEMs respectively. PEM thickness as a function of the number of bilayers, measured by optical waveguide light mode spectroscopy (OWLS) for (PEI-(PSS/PAH)i (circles) or PEI–(PGA/PLL)i (squares) (2).

conductivity, or photosensitivity[6] of a surface through appropriate material selection and optimization of the assembly procedure.

Polyelectrolyte molecular weight (MW) can be important when assembling PEMs, especially if the polyelectrolyte has a particularly low MW. While high MW polyelectrolytes build up in a linear growth mode, lower MW polyelectrolytes have exhibited an exponential growth mode, i.e., the thickness increase is greater for each subsequent layer (Fig. 1).[2]

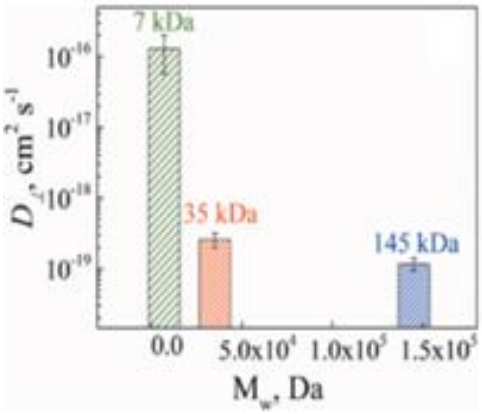

Figure 2: Diffusion coefficients perpendicular to the substrate of various MWs of PMAA chains (13).

One explanation for this exponential growth of low MW polyelectrolytes is diffusion into the PEMs leading to the formation of polyanion/polycation complexes. Linearly growing PEMs have been observed to have a mostly layered structure with some interpenetration between layers.[11,12] It has been shown that diffusion is more favorable for low MW polymers (Fig. 2).[13] Since lower MW polyelectrolytes are more mobile than their higher MW counterparts, they are able to diffuse further into the multilayer and to balance the chemical potential by creating polyanion/polycation complexes.[2] These complexes contribute the additional mass and thickness that characterizes exponential growth in lower MW PEMs.

Some research has suggested that low MW polyelectrolytes may not improve growth, but rather lead to a plateau in growth. While the addition of polyelectrolytes to an assembling PEM is expected to form the next layer (Fig. 3b),[7] they can instead strip molecules off the surface (Fig. 3a). To continue building the PEM, the adhesion of polyelectrolytes must be more favorable than the stripping process. The occurrence of polyelectrolytes stripping off after adhering (Fig. 3c) must not be significant on the timescale used for layer build up. A study by Sui et al. reported that some PEMs with a low MW polyelectrolyte exhibit stripping, characterized by a plateau and subsequently a decrease in thickness.[7] It is possible that this is an indication that these polyelectrolytes have a low diffusivity and are therefore unable to form complexes before stripping molecules off the PEM.[2] It is important to characterize the assembly pattern to assess the influence of the growth mode on the surface properties of the resulting PEM.

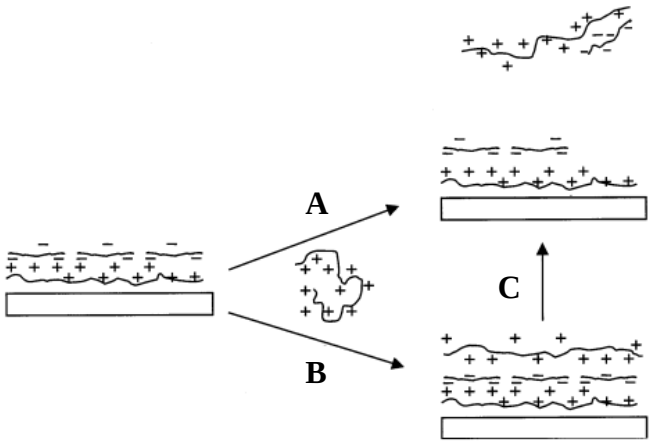

Figure 3: Sticking versus stripping when adding polyelectrolytes to low molecular weight layers. (A) The adhesion between the added polyelectrolyte and one or more molecules of the previous layer can be stronger than the bonds within the existing layers, allowing mass to be stripped off. (B) The added polyelectrolyte can adhere and form a part of the next layer, as intended. (C) Some polyelectrolytes can at first adhere, and then strip off. Adapted from (7).

2.2 Surface Properties

PEMs are often used as a coating on a structure to modify its surface properties[6] including surface free energy and roughness. Therefore, significant research on PEMs has been directed towards optimizing their assembly to control for surface properties relevant to the specific use of the PEM.

Surface free energy (SFE), the excess of energy at the surface of a given material, is an important property of PEMs to control. One way to observe the SFE is through the contact angle, or wettability. When a droplet of liquid contacts a surface, a high free energy surface will be more wettable, as the liquid has an energetic incentive to increase the area of contact with the surface. This can be measured using the contact angle between the liquid and surface, while taking into consideration the surface tension of the liquid.[14] The SFE of a PEM can have a significant effect on the hydrophobicity[15] and cell adhesion,[16] as well as other properties that are adjusted for specific applications.

Roughness is also an important property to consider when designing PEMs. Roughness describes the variations in the surface profile of a material and can be quantified using atomic force microscopy (AFM). Roughness can be adjusted in PEMs for various applications, including optical applications that require a smooth surface.[17]

There has been limited research on the effect that MW and growth mode have on surface properties, including surface free energy and roughness. Kujawa et al. have shown that PEMs created from low MW are rougher.[18] Solomaki et al. compared poly(allylamine hydrochloride) (PAH)/poly(acrylic acid) (PAA) PEMs with either both low MW or both high MW polyelectrolytes and in each condition measured the advancing water contact angle. They found that low MW PAH produced a surface with a higher water contact angle, while low MW PAA usually yielded a lower water contact angle (Fig. 4).[19] Additional research is needed to understand the role that molecular weight plays in the surface properties of polyelectrolyte multilayers, as this will allow for greater design control of these critical properties.

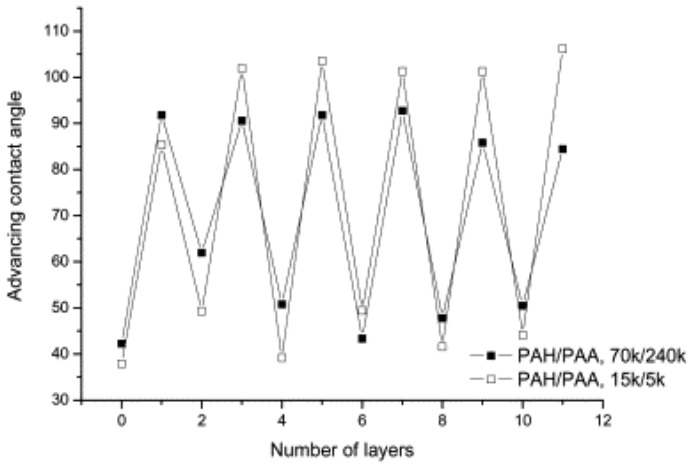

Figure 4: Advancing water contact angle in low and high molecular weight PAH/PAA PEMs (19).

3. Methods

3.1 Research Strategy

This research endeavor explored the relationship between the molecular weight of the polyelectrolytes and the surface properties of the PEMs including surface roughness and surface free energy. The results of this study will allow for greater prediction and control of PEM surface properties.

3.2 Materials

PAA with molecular weights of 1.8k, 100k, 250k and poly-l-lysine (PLL) with molecular weights 15-30k, 120k, and 275k were used. Three different conditions were studied: PAA (MW 1.8k)/PLL (MW 15-30k), PAA (MW 100k)/PLL (MW 120k), and PAA (MW 250k)/PLL (MW 275k). These are referred to in this study as low, medium, and high MW, respectively. Low and high MW polyelectrolytes were not combined to form PEMs to avoid the stripping mechanism.

3.3 Assembly

PEMs were assembled on a quartz substrate with a 100 nm gold coating using 1 mg/mL solutions of each polyelectrolyte. Solutions were adjusted to a pH of 6.0. Each layer was allowed to adsorb for 15 minutes followed by two 1.5 minute wash steps with DI water. A layer of PAA was assembled, followed by a layer of PLL, and then alternating layers were added until a total of 10 bilayers were formed. To observe the assembly pattern, PEMs with fewer bilayers were assembled and characterized.

3.4 Characterization

Quartz Crystal Microbalance with Dissipation Monitoring

The changes in mass were measured using quartz crystal microbalance with dissipation monitoring (QCM-D), a common technique for thin film analysis.[20,21] Mass changes were calculated from their relationship with recorded shifts in the resonant frequency and energy dissipation of the QCM-D sensor. The Sauerbrey equation (Eq. 1) can be used for rigid films, where Δf is the frequency change, f_0 is the resonant frequency, A is the surface area of the quartz crystal, ρ_q is the density of the crystal, μ_q is the shear modulus of the crystal, and finally Δm is the change in mass of the film.

$$\Delta f = \frac{2f_0^2}{A\sqrt{\rho_q \mu_q}} \Delta m \qquad \text{Equation 1}$$

Therefore, by recording the changes in frequency and energy dissipated as the PEM is assembled, the mass deposited was monitored. Changes in frequency and dissipation were measured continuously deposited and converted to mass changes using the Sauerbrey equation. The change of energy dissipation (ΔD) was also measured to account for the viscoelastic properties of the film, as the Sauerbrey equation would otherwise underestimate the mass of insufficiently

rigid films. By considering the ratio of ΔD to Δ*f*, the stiffness was evaluated for each condition. Finally, frequency and dissipation can be measured at different overtones, indicating the number of nodal planes parallel to the surface. Measurements were compared between overtones to provide insight into the cross-sectional structure of the PEMs.

The mass deposited was measured using a Q-Sense E4 (Biolin Scientific) on QSX 301 gold sensors. Each polyelectrolyte solution (1 mg/mL) was flowed at a constant rate of 50 µL/min for 15 minutes for each adhered layer, followed by a 10-minute rinse of DI water. Four measurements were taken for each condition.

Spectroscopic Ellipsometry

The thickness of the PEMs was measured at various points in their assembly to characterize their assembly pattern. Ellipsometry was used to calculate the changes in thickness by measuring the change in amplitude and phase of polarized light that reflects or transmits from the PEM. The model was calculated using the fitting parameters amplitude ratio (Ψ) and phase difference (Δ). A multi-wavelength Spectroscopic Ellipsometer (SE) system (J. A. Woollam Co.) was used to measure the thickness at various bilayer intervals. A Cauchy layer on top of a gold substrate was used to fit data with wavelengths between 300-800 nm. Measurements were taken at 65°, 70°, and 75° at three random locations on three samples, totaling nine measurements for each condition.

Relative Density

The ratio of the mass deposited measured with QCM-D and the thicknesses determined with ellipsometry were considered to yield a relative density for each condition.

Goniometry

The SFE of each PEM was analyzed by measuring the static contact angle with water, n-heptane, chloroform, ethylene glycol, and glycerol. The van Oss, Good, Chaudhury (VGC) approach will be used to determine the SFE of each multilayer. This method considers the SFE (γ) to be composed of a dispersive component (γ^d) and a polar component (γ^p) which can be further broken down into an acidic (γ^+) and basic component (γ^-) (Eq. 2).[22]

$$\gamma = \gamma^d + \gamma^p = \gamma^d + 2\sqrt{\gamma^+\gamma^-}$$

Equation 2

The contact angle (θ) can be used to determine the SFE of each multilayer (γ_s) by using the known component surface energies of each liquid (Eq. 3,[22] Table 1).

$$\frac{\gamma_l(1+\cos(\theta)) - 2\sqrt{\gamma_l^d\gamma_s^d}}{2\sqrt{\gamma_l^-}} = \sqrt{\gamma_s^+} + \sqrt{\frac{\gamma_l^+\gamma_s^-}{\gamma_l^-}}$$

Equation 3

Table 1: Surface Tension of Liquids (mJ/m^2) at 20°C[23]

Liquid	Formula	Total SFE (γ)	Dispersive (γ^d)	Polar (γ^p)	Acidic (γ^+)	Basic (γ^-)
Water	H_2O	72.8	21.8	51	25.5	25.5
n-Heptane	C_7H_{16}	20.1	20.1	0	0	0
Chloroform	$CHCl_3$	27.2	27.2	0	1.5	0
Ethylene Glycol	$C_2H_6O_2$	48	29	19	3	30.1
Glycerol	$C_3H_8O_3$	64	34	30	3.92	57.4

This measurement was conducted with a contact angle goniometer (Ramé-Hart) for various bilayer intervals. For each condition, measurements were taken in three random locations on three samples, totaling nine measurements.

Atomic Force Microscopy

The roughness of PEM surfaces was measured using a Nanosurf NaioAFM instrument for various bilayer intervals. The AFM measurements were taken under constant force mode, using a CSC17 probe. These measurements were used to calculate the roughness average (R_a) from n ordered, equally spaced points at a vertical distance of y from the mean line (Eq. 4).

$$R_a = \frac{1}{n}\sum_{i=1}^{n} |y_i| \qquad \text{Equation 4}$$

For each condition, measurements were taken in three random locations on three samples, totaling nine measurements.

3.5 Statistical Analysis

In the following section, error bars are an indication of the 95% confidence interval.

5. Results and Discussion

5.1 Assembly Pattern

Mass and Composition

The mass of each PEM was monitored as the layers assembled to provide insight about the growth pattern produced by each combination of polyelectrolytes (Fig 7). As molecular weight of the polyelectrolytes increased, PEMs were more massive. In the low MW PEMs, adding PAA solution initially increased the mass, but began to strip mass off after the second bilayer. This continued until the mass of the PEMs plateaued by approximately 6 bilayers, as the addition of mass from PLL barely surpassed the lost mass.

The high MW PEMs grew in an exponential pattern, primarily due to the contributions of PAA. The mass added by PAA per layer increased significantly with the layer number, while the contribution per layer from PLL increased to a point, but then decreased with the layer number to the extent that some trials observed stripping in the final bilayer (Fig. 5).

The medium MW PEMs assembled a much more balanced and consistent composition, though PLL contributed slightly more mass to each layer (Fig. 5). Especially after the second bilayer, these PEMs demonstrated a linear growth pattern (Fig. 7).

The assembled mass was also compared between overtones by examining the changes in frequency. An overtone with a lower number indicates that the measurement is taken further from the substrate. In each condition, more mass was assembled at lower overtones, meaning more mass was assembled further from the substrate (Fig 6). This trend was more significant as MW of the polyelectrolytes increased, and as the layer number increased. (Fig 6, 8).

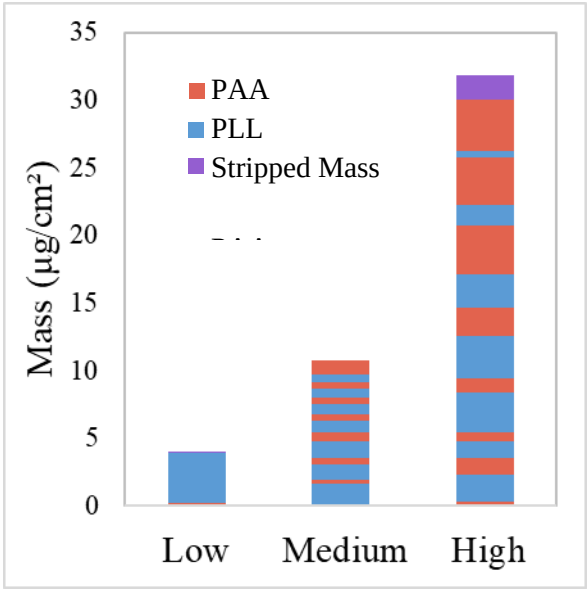

Figure 6: Composition by polyelectrolyte of PAA-PLL PEMs. Low MW PAA-PLL (1.8kDa and 15-30kDa), Medium MW PAA-PLL (100kDa and 120kDa), High MW PAA-PLL (250kDa and 275kDa) are displayed, with earlier layer at the bottom of the graph. The full extent of stripping in Low MW PEMs can be seen in Appendix A.

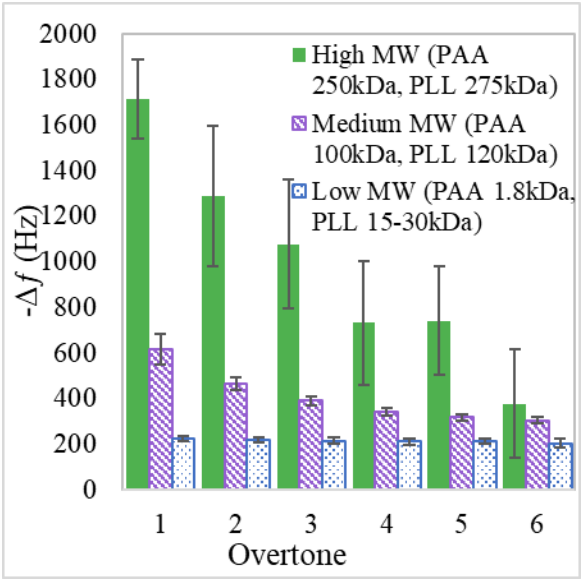

Figure 5: Change in frequency of PAA-PLL PEMs at various overtones.

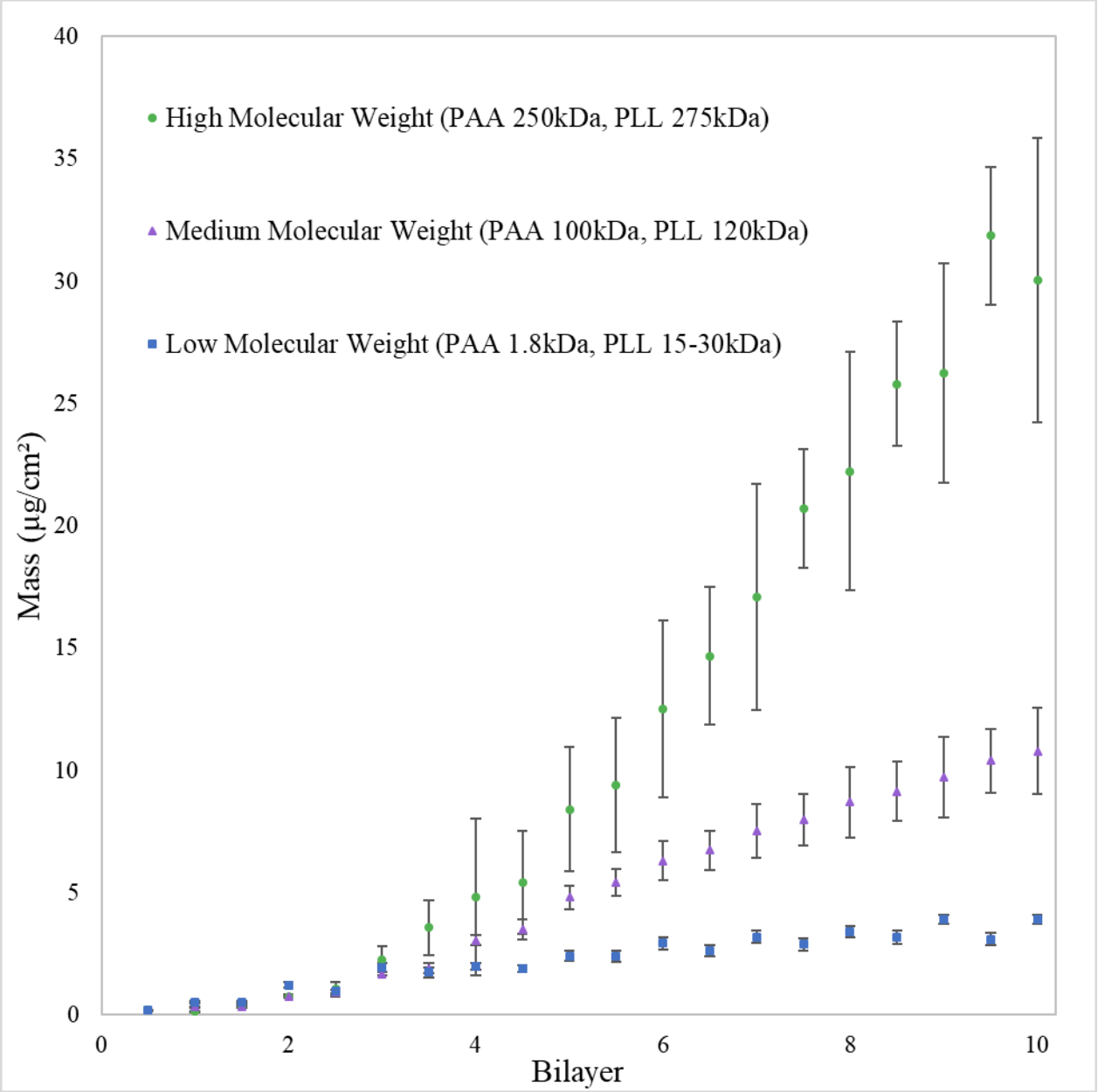

Figure 7: Assembled mass of PAA-PLL PEMs. Mass was calculated from continuous measurements of the frequency of the third overtone using QCM-D; rather than depict the continuous mass, a value was chosen for each layer at the end of the wash, immediately before the next layer began.

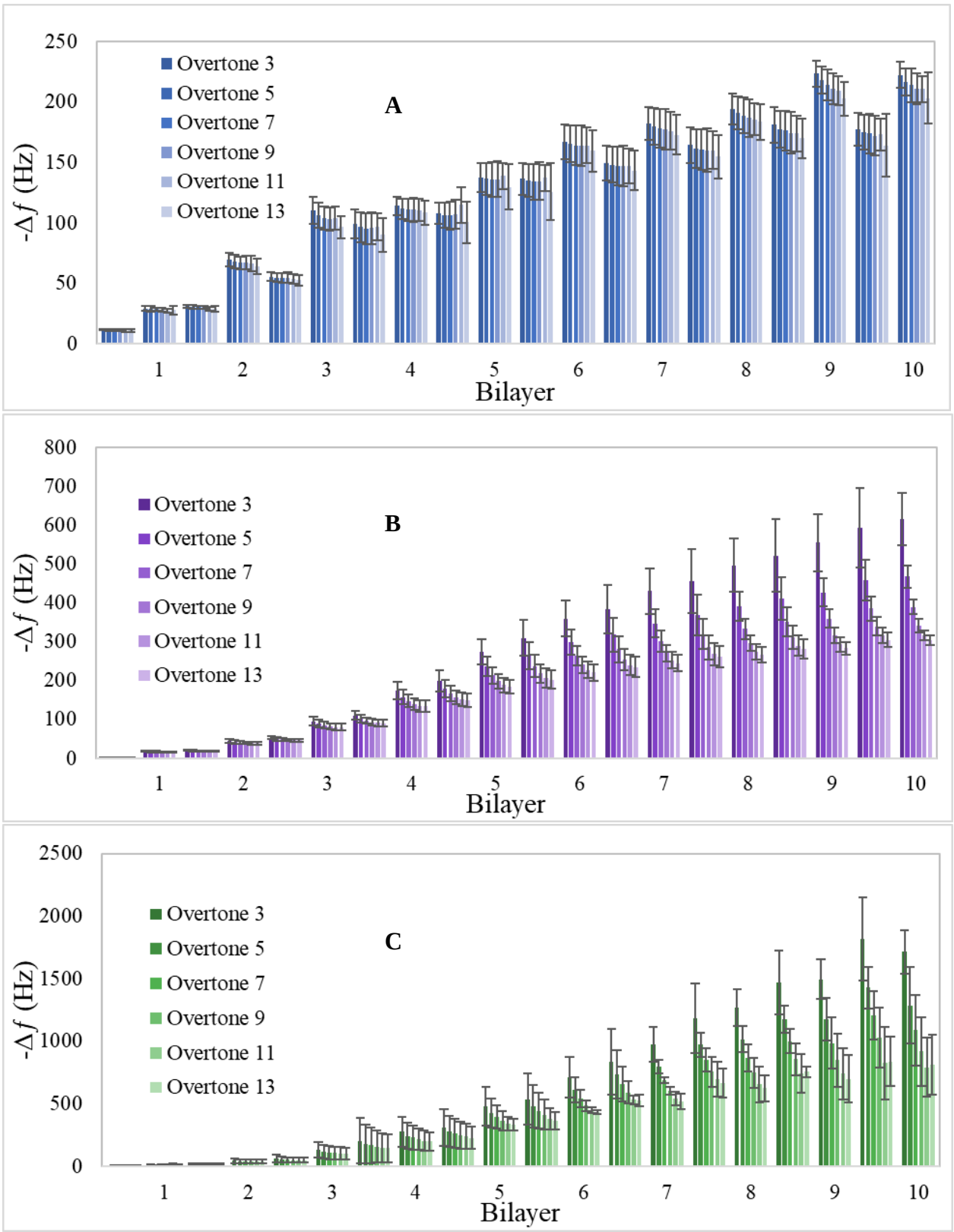

Figure 8: Change in frequency of PAA-PLL PEMs at various overtones at each layer. (A) Low MW PAA-PLL (1.8kDa and 15-30kDa), (B) Medium MW PAA-PLL (100kDa and 120kDa), (C) High MW PAA-PLL (250kDa and 275kDa)

Thickness and Relative Density

The thickness of each PEM was measured at several intervals during assembly (Fig 9). The data was fit to a modified Cauchy layer, where the absorption constant was adjusted to better match the data of each of the three conditions. All three conditions showed slow initial growth, with medium MW PEMs becoming the thickest. By comparing the ratio of the mass assembled and the thickness of each film, the density of each PEM can be evaluated. It should be noted, however, that these can only be considered to be relative densities, as thickness measurements were taken on dry sample while QCM-D results are from PEMs immersed in an aqueous environment. All conditions exhibited an increase in density as layers were added until a plateau between bilayers 3-8 and finally a decreased density at the final layer (Fig. 10).

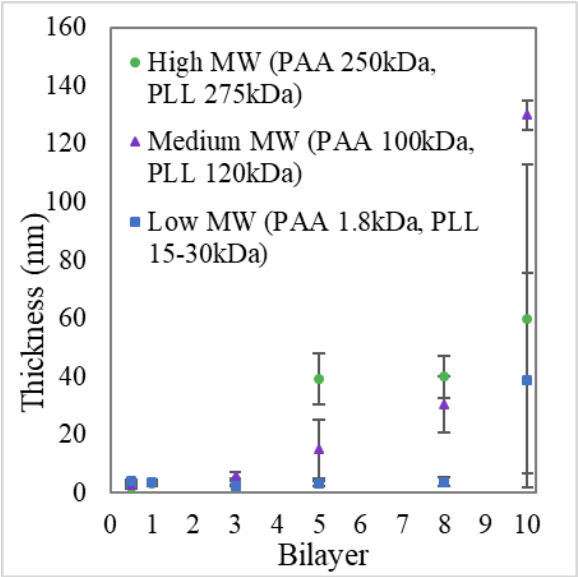

Figure 9: Thickness of PAA-PLL PEMs.

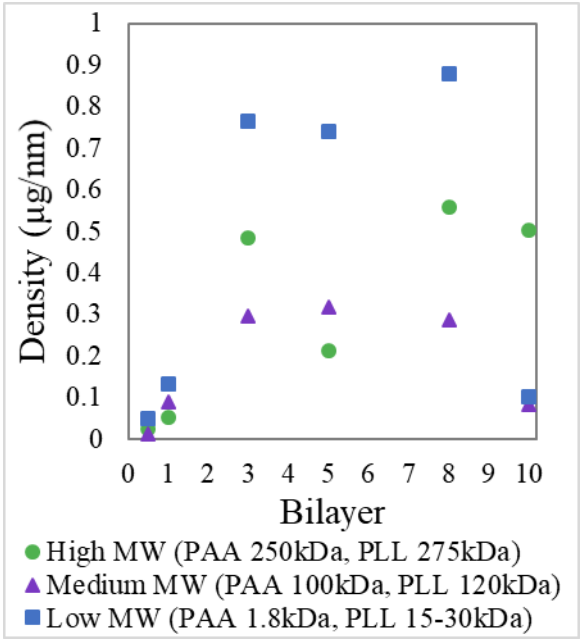

Figure 10: Relative density of PAA-PLL PEMs.

Stiffness

The stiffness of each PEM was evaluated using the ratio of dissipation change to frequency change $\left({}^{\Delta D}/_{\Delta f}\right)$ where a lower value indicates a stiffer film. Low MW PEMs were an order of magnitude stiffer than medium or high MW PEMs, which did not show a significant difference, though high MW PEMs were slightly stiffer (Table 2). The stiffness did not vary extremely between overtones, suggesting all PEMs had similar stiffness at various distances from the substrate (Fig. 11). Low MW PEMs were stiffest in the center (Fig. 11a), while medium MW PEMs are least stiff in the center (Fig. 11b), and high MW PEMs are stiffest at the substrate (Fig. 11c). Refer to Appendix B for additional data on the stiffness of these films.

Table 2: Stiffness of PAA-PLL Multilayers

MW	Average $\frac{\Delta D}{\Delta F}$	95% Confidence Interval
Low	0.036	0.019-0.053
Medium	0.33	0.24-0.41
High	0.31	0.14-0.48

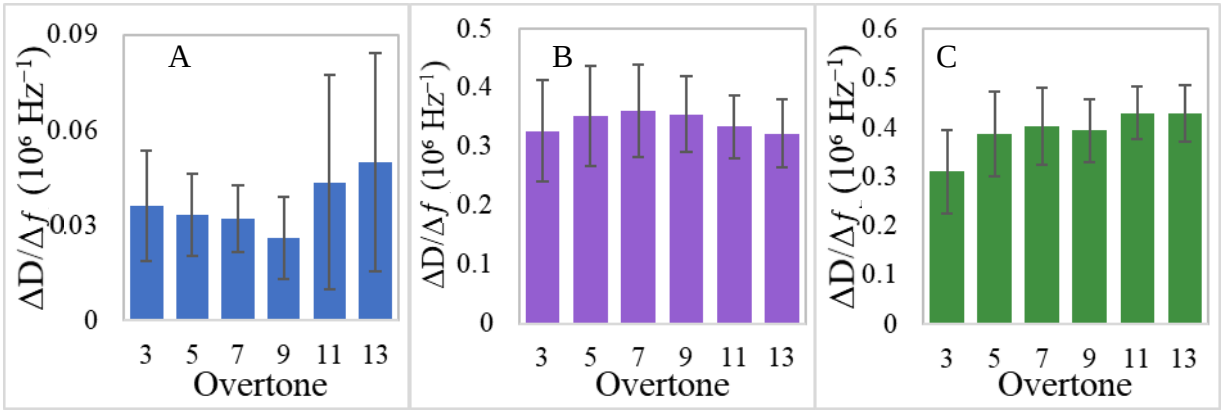

Figure 11: Stiffness of PAA-PLL PEMs at various overtones as shown by ΔDissipation/ΔFrequency. (A) Low MW PAA-PLL (1.8kDa and 15-30kDa), (B) Medium MW PAA-PLL (100kDa and 120kDa), (C) High MW PAA-PLL (250kDa and 275kDa)

5.2 Surface Roughness

Atomic force microscopy was used to measure the roughness average (R_a) of each PEM at various stages in assembly. All PEMs demonstrated an increase in roughness as more layers were added. Low MW PEMs were the roughest, followed by high MW PEMs, and then medium MW PEMs (Fig 11). PEMs exhibited certain topographies based on the molecular weight of their constituent polyelectrolytes. Medium MW PEMs had sharp peaks of polymer aggregates that were lower than those in low or high MW PEMs. Both low and high MW PEMs had broader and taller peaks, but individual high MW peaks seemed to be smoother, while the low MW PEM seemed to have peaks upon peaks.

These results demonstrate the impact of the molecular weight, and therefore assembly pattern, on surface roughness. Among the three MWs tested, the medium MW PEMs seem to represent a good balance between the extreme behaviors of both low and high MW PEMs. The comparatively balanced composition, steady growth rate, and consistent density may have led to a more homogenous and smooth surface.

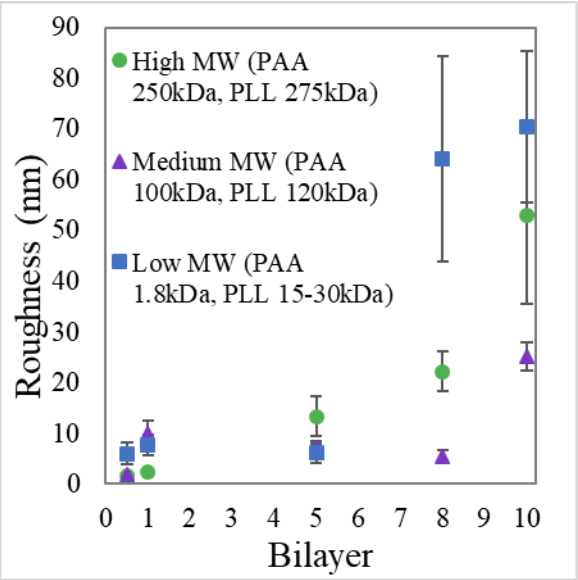

Figure 12: Roughness (Rms) of PAA-PLL PEMs.

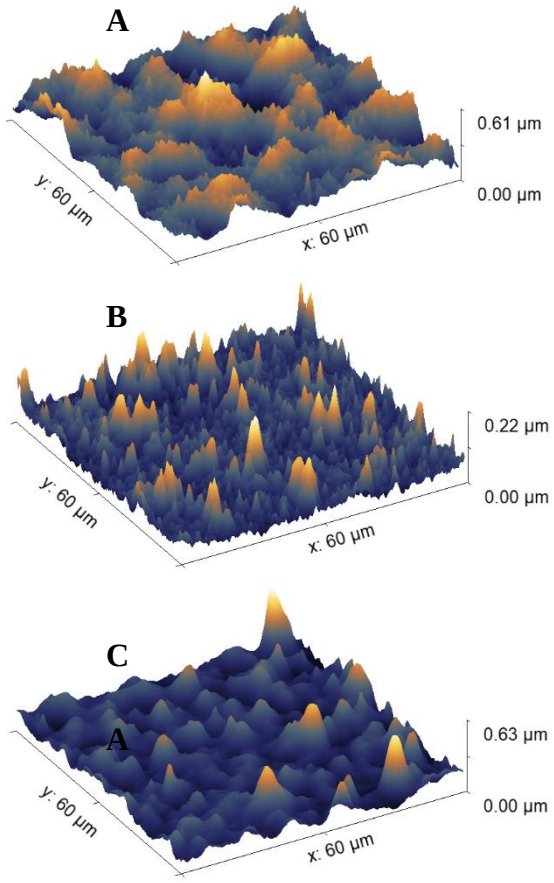

Figure 13: Representative topography of PAA-PLL PEMs with 10bL. (A) Low MW PAA-PLL (1.8kDa and 15-30kDa), (B) Medium MW PAA-PLL (100kDa and 120kDa), (C) High MW PAA-PLL (250kDa and 275kDa). Note that the Z-scale of (B), as these peaks were quite a bit smaller than those of (A) or (C).

5.3 Surface Free Energy

The contact angle was measured for five liquids, and the VCG method was used to determine the component SFE of each PEM. Low MW PEMs were found to have the highest SFE (Fig. 14), dominated by the higher basic surface free energy (Fig. 15c). This may be related to the basic properties of PLL coupled with the increased PLL ratio in low MW PEMs. However, the low MW PEMs had a comparatively low dispersive SFE (Fig 15a). While medium MW PEMs had the lowest SFE overall, they were very similar to high MW PEMs. Both medium and high MW PEMs steadily dropped in basic SFE as they were assembled, while their dispersive SFE generally increased.

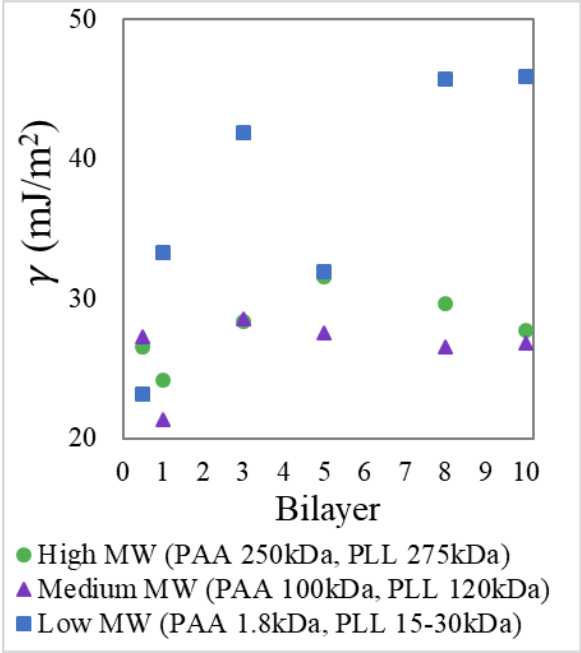

Figure 14: Total surface free energy of PAA-PLL PEMs

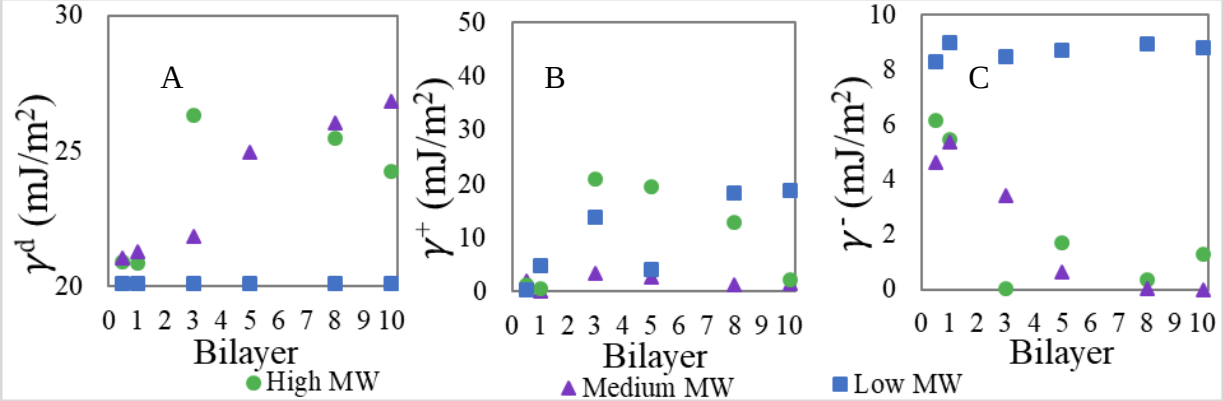

Figure 15: Component surface free energy of PAA-PLL PEMs. (A) Dispersive, (B) Acidic, and (C) Basic components.

6. Conclusion

In PAA-PLL PEMs, there are several ways that MW affects surface properties. This research demonstrated that there may be an optimal range of medium MWs that produces the smoothest surfaces with the lowest SFE. While further research would be needed to assess both the specific range and the cause of this pattern, it may be related to the linear growth pattern in these medium MW PEMs, which had the most balanced composition by polyelectrolyte among the conditions studied. Alternatively, low MW polyelectrolytes can be used to form rougher films with higher SFE. Specifically, these PEMs have a high basic component to their SFE, possibly attributable to their high PLL content. Finally, high MW polyelectrolytes were found to create rough films with low SFE. These results display the tunability of PEMs and their surface properties using molecular weight.

References

(1) Decher, G.; Hong, J. D.; Schmitt, J. Buildup of Ultrathin Multilayer Films by a Self-Assembly Process: III. Consecutively Alternating Adsorption of Anionic and Cationic Polyelectrolytes on Charged Surfaces. *Thin Solid Films* **1992**, *210*, 831–835.

(2) V Klitzing, R. Internal Structure of Polyelectrolyte Multilayer Assemblies. *Phys. Chem. Chem. Phys.* **2006**, *8* (43), 5012–5033.

(3) Xu, Y.; Xu, C.; Shvarev, A.; Becker, T.; De Marco, R.; Bakker, E. Kinetic Modulation of Pulsed Chronopotentiometric Polymeric Membrane Ion Sensors by Polyelectrolyte Multilayers. *Anal. Chem.* **2007**, *79* (18), 7154–7160.

(4) Lulevich, V. V.; Nordschild, S.; Vinogradova, O. I. Investigation of Molecular Weight and Aging Effects on the Stiffness of Polyelectrolyte Multilayer Microcapsules. *Macromolecules* **2004**, *37* (20), 7736–7741.

(5) Daubiné, F.; Cortial, D.; Ladam, G.; Atmani, H.; Haïkel, Y.; Voegel, J. C.; Clézardin, P.; Benkirane-Jessel, N. Nanostructured Polyelectrolyte Multilayer Drug Delivery Systems for Bone Metastasis Prevention. *Biomaterials* **2009**, *30* (31), 6367–6373.

(6) Bertrand, P.; Jonas, A.; Laschewsky, A.; Legras, R. Ultrathin Polymer Coatings by Complexation of Polyelectrolytes at Interfaces: Suitable Materials, Structure and Properties. *Macromol. Rapid Commun.* **2000**, *21* (7), 319–348.

(7) Sui, Z.; Salloum, D.; Schlenoff, J. B. Effect of Molecular Weight on the Construction of Polyelectrolyte Multilayers: Stripping versus Sticking. *Langmuir* **2003**, *19* (6), 2491–2495.

(8) Sukhorukov, G. B.; Donath, E.; Lichtenfeld, H.; Knippel, E.; Knippel, M.; Budde, A.; Möhwald, H. Layer-by-Layer Self Assembly of Polyelectrolytes on Colloidal Particles. *Colloids Surfaces A Physicochem. Eng. Asp.* **1998**, *137* (1–3), 253–266.

(9) Caruso, F.; Caruso, R. A.; Möhwald, H.; Caruso, F.; Caruso, R. A.; Mohwald, H. Nanoengineering of Inorganic and Hybrid Hollow Spheres by Colloidal Templating Published by : American Association for the Advancement of Science Stable URL : http://www.jstor.org/stable/2897357 Nanoengineering of Inorganic and Hybrid Hotlow Spheres by Co. **1998**, *282* (5391), 1111–1114.

(10) Neff, P. A.; Naji, A.; Ecker, C.; Nickel, B.; Klitzing, R. V.; Bausch, A. R. Electrical Detection of Self-Assembled Polyelectrolyte Multilayers by a Thin Film Resistor. *Macromolecules* **2006**, *39* (2), 463–466.

(11) Schmitt, J.; Grünewald, T.; Decher, G.; Pershan, P. S.; Kjaer, K.; Lösche, M. Internal Structure of Layer-by-Layer Adsorbed Polyelectrolyte Films: A Neutron and X-Ray Reflectivity Study. *Macromolecules* **1993**, *26* (25), 7058–7063.

(12) Jomaa, H. W.; Schlenoff, J. B. Salt-Induced Polyelectrolyte Interdiffusion in Multilayered Films: A Neutron Reflectivity Study. *Macromolecules* **2005**, *38* (20), 8473–8480.

(13) Selin, V.; Ankner, J. F.; Sukhishvili, S. A. Diffusional Response of Layer-by-Layer Assembled Polyelectrolyte Chains to Salt Annealing. *Macromolecules* **2015**, *48* (12), 3983–3990.

(14) Williams, D. *Essential Biomaterials Science*; Cambridge University Press, 2014.

(15) Wang, L.; Wei, J.; Su, Z. Fabrication of Surfaces with Extremely High Contact Angle Hysteresis from Polyelectrolyte Multilayer. *Langmuir* **2011**, *27* (24), 15299–15304.

(16) Kovačević, D.; Pratnekar, R.; Torkar, K. G.; Salopek, J.; Dražić, G.; Abram, A.; Bohinc, K. Influence of Polyelectrolyte Multilayer Properties on Bacterial Adhesion Capacity. *Polymers (Basel).* **2016**, *8* (10).

(17) Ghostine, R. A.; Jisr, R. M.; Lehaf, A.; Schlenoff, J. B. Roughness and Salt Annealing in a Polyelectrolyte Multilayer. *Langmuir* **2013**, *29* (37), 11742–11750.

(18) Kujawa, P.; Moraille, P.; Sanchez, J.; Badia, A.; Winnik, F. M. Effect of Molecular Weight on the Exponential Growth and Morphology of Hyaluronan/chitosan Multilayers: A Surface Plasmon Resonance Spectroscopy and Atomic Force Microscopy Investigation. *J. Am. Chem. Soc.* **2005**, *127* (25), 9224–9234.

(19) Salomäki, M.; Vinokurov, I. A.; Kankare, J. Effect of Temperature on the Buildup of Polyelectrolyte Multilayers. *Langmuir* **2005**, *21* (24), 11232–11240.

(20) Lyu, X.; Peterson, A. M. The Princess and the Pea Effect: Influence of the First Layer on Polyelectrolyte Multilayer Assembly and Properties. *J. Colloid Interface Sci.* **2017**, *502*, 165–171.

(21) Naderi, A.; Claessont, P. M. Adsorption Properties of Polyelectrolyte-Surfactant Complexes on Hydrophobic Surfaces Studied by QCM-D. *Langmuir* **2006**, *22* (18), 7639–7645.

(22) Boerio, F. J. Interfacial Energies and Their Role in Adhesion. In *The Adhesion Society Short Course "Adhesion Theory and Practice";* Savannah, GA, 2011.

(23) van Oss, C. J. *Interfacial Forces in Aqueous Media*, 2nd ed.; CRC Press: Boca Raton, FL, 2006.

Appendices

Appendix A: Expanded Composition of Low MW PEMs

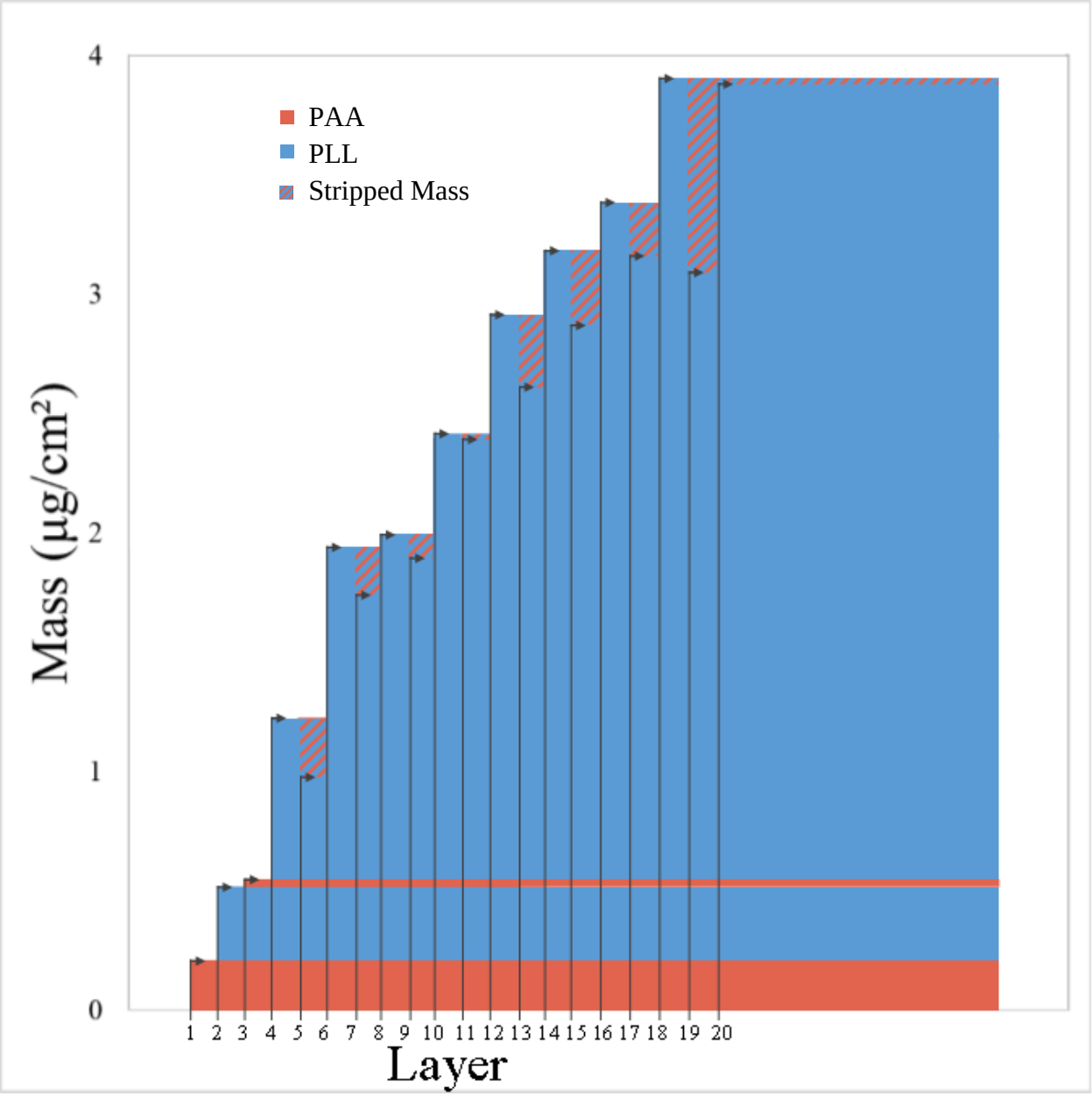

Figure 16: Expanded composition by polyelectrolyte of low MW PEMs. This expanded figure demonstrates that the stripping is significantly more extensive than can be seen in Figure 6 for low MW (1.8kDa PAA and 15-30kDa PLL) PEMs.

Appendix B: Supplementary Figures for Stiffness

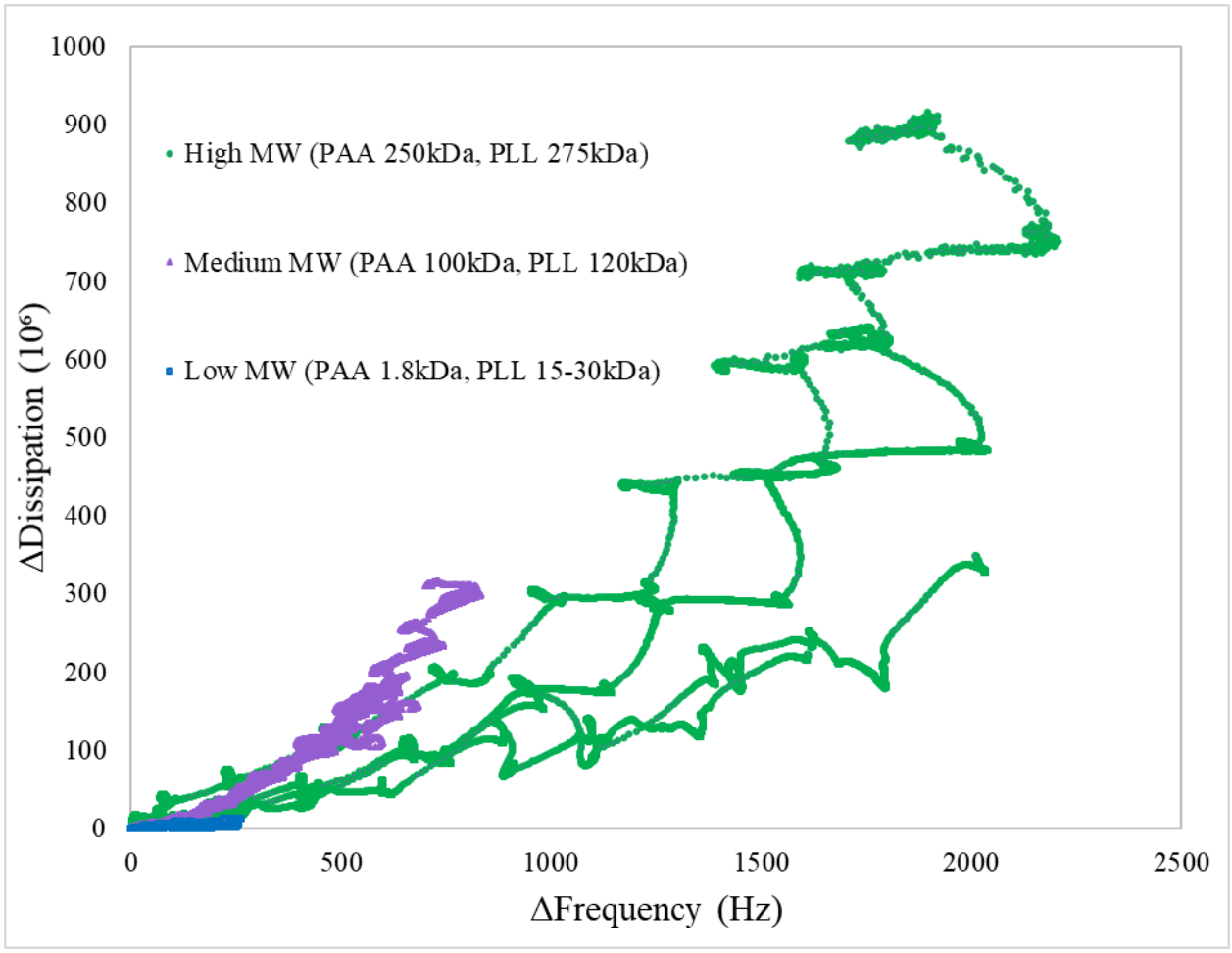

Figure 17: Stiffness of PAA-PLL PEMs as shown by ΔDissipation/ΔFrequency.

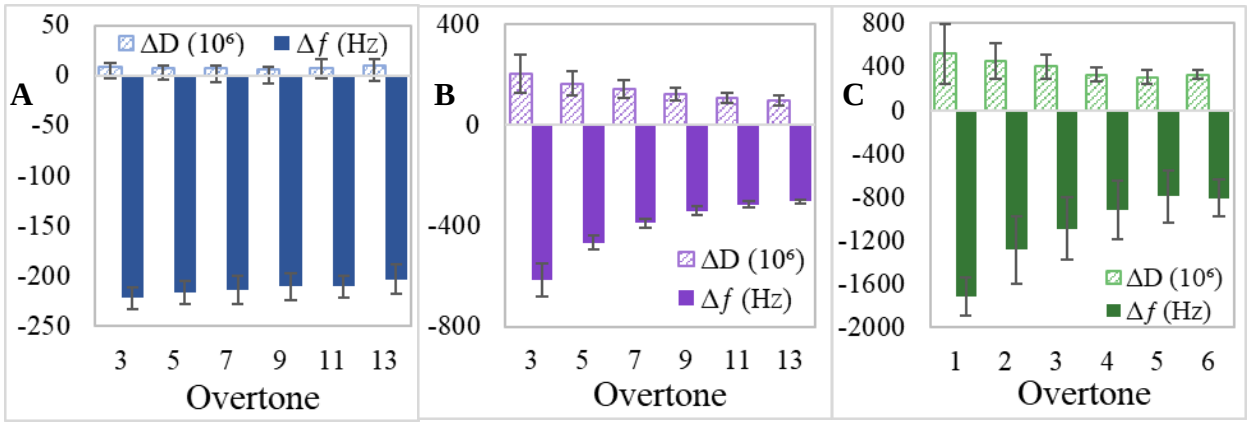

Figure 18: Frequency and dissipation of PAA-PLL PEMs at various overtones. (A) Low MW PAA-PLL (1.8kDa and 15-30kDa), (B) Medium MW PAA-PLL (100kDa and 120kDa), (C) High MW PAA-PLL (250kDa and 275kDa).

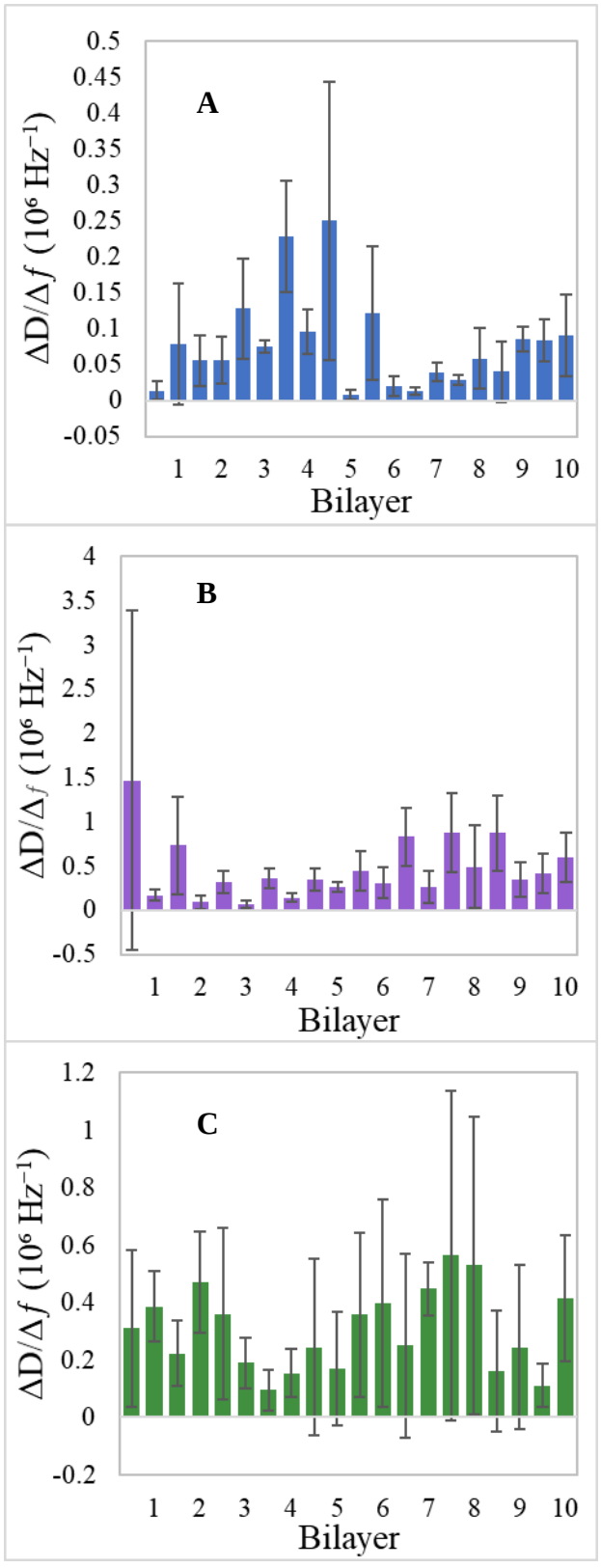

Figure 20: Stiffness of PAA-PLL PEMs as shown by ΔDissipation/ΔFrequency. (A) Low MW PAA-PLL (1.8kDa and 15-30kDa), (B) Medium MW PAA-PLL (100kDa and 120kDa), (C) High MW PAA-PLL (250kDa and 275kDa).

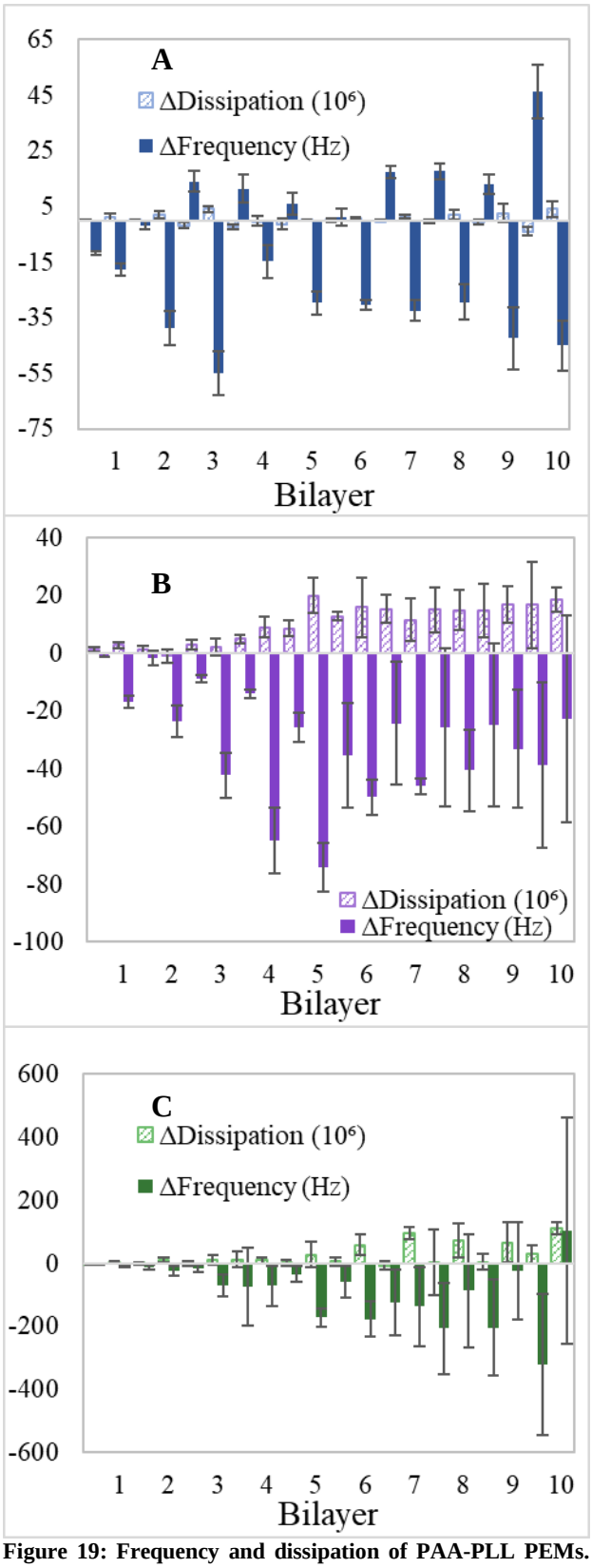

Figure 19: Frequency and dissipation of PAA-PLL PEMs. (A) Low MW PAA-PLL (1.8kDa and 15-30kDa), (B) Medium MW PAA-PLL (100kDa and 120kDa), (C) High MW PAA-PLL (250kDa and 275kDa).